

Investigation on the Flexural Creep Stiffness Behavior of PC–ABS Material Processed by Fused Deposition Modeling Using Response Surface Definitive Screening Design

OMAR AHMED MOHAMED^{1,3}, SYED HASAN MASOOD,¹
and JAHAR LAL BHOWMIK²

1.—Department of Mechanical and Product Design Engineering, Swinburne University of Technology, Hawthorn, VIC, Australia. 2.—Department of Statistics, Data Science and Epidemiology, Swinburne University of Technology, Hawthorn, VIC, Australia. 3.—e-mail: Omar.Ahmed.Mohamed@outlook.com

The resistance of polymeric materials to time-dependent plastic deformation is an important requirement of the fused deposition modeling (FDM) design process, its processed products, and their application for long-term loading, durability, and reliability. The creep performance of the material and part processed by FDM is the fundamental criterion for many applications with strict dimensional stability requirements, including medical implants, electrical and electronic products, and various automotive applications. Herein, the effect of FDM fabrication conditions on the flexural creep stiffness behavior of polycarbonate–acrylonitrile–butadiene–styrene processed parts was investigated. A relatively new class of experimental design called “definitive screening design” was adopted for this investigation. The effects of process variables on flexural creep stiffness behavior were monitored, and the best suited quadratic polynomial model with high coefficient of determination (R^2) value was developed. This study highlights the value of response surface definitive screening design in optimizing properties for the products and materials, and it demonstrates its role and potential application in material processing and additive manufacturing.

INTRODUCTION

With the increasing use of the fused deposition modeling (FDM) additive manufacturing process in several engineering areas such as the aerospace, electrical, electronic, automotive, and industrial sectors, it is necessary to determine and evaluate the stress and deformation to predict the reliability and failure behavior of the manufactured products by this process. The material properties are highly influenced by the FDM fabrication conditions, and these are difficult to characterize because of the strong parametric interactions.¹ To extend the industrial applications of the FDM process, greater attention is required on the manufacturing process and on control of the fabrication parameters, which influence the properties of the final products.² Creep in the thermoplastic materials is a complex phenomenon, which depends on both thermoplastic material properties and external conditions.³ In

practical applications, the functionality of the manufactured parts and the material processed by FDM technology and their responses to the loading and stress over time strongly depend on the processing parameters used at the time of fabrication. Generally, polymers are characterized by the creep phenomenon, which affects the mechanical performance and the material application in long-term reliability and durability of the manufactured parts.⁴ It is well known that the thermoplastic materials can produce high deformation and creep rates after releasing the applied load. If the material and the part processed by FDM technology has been used in inappropriate application as a result of lack of knowledge, the thermoplastic materials would suffer unrecovered deformation, resulting in dimensional instability and leading to premature failure. Therefore, flexural creep stiffness of the part processed by FDM should be really considered in practical applications.

Recent studies have reported that the FDM process parameters can cause major quality-related issues such as interlayer cracking, micro-voids, distortion, and warpage. For example, Hossain et al.⁵ studied the effect of various process parameters such as raster angle, contour width, raster width, and raster-to-raster air gap on the ultimate tensile strength of FDM-manufactured polycarbonate parts. Torres et al.⁶ performed experiments on FDM components made from polylactic acid (PLA) using a Taguchi L⁹ orthogonal array to optimize the mechanical properties such as part strength and ductility. They also addressed how to compromise between optimum process settings for part strength and ductility simultaneously. Knoop and Schoeppner⁷ measured and compared the tensile strength, Young's modulus, elongation at break, flexural strength, and compressive strength of the FDM polyamide with 12 samples fabricated in two different build orientations and layer thicknesses. The results showed that the anisotropy in polyamide samples is not as strong as for other FDM materials. Basavaraj and Vishwas⁸ investigated the impact of FDM process conditions on tensile strength and dimensional accuracy of Nylon using the Taguchi method. They concluded that the layer thickness is the most influential factor on the tensile strength and dimensional accuracy. Mohamed et al.⁹ formulated mathematical models for build time, material consumption, and dynamic flexural modulus of FDM-processed polycarbonate–acrylonitrile-butadiene-styrene (PC–ABS) prototypes using Q-optimal design and obtained the optimal process conditions. Griffiths et al.¹⁰ demonstrated how experimental design and statistical analysis can be used to improve the mechanical properties of the materials as well as the build quality. It was shown that the layer thickness has an insignificant effect on the tensile strength, but it has a significant impact on build time and material usage. Es-Said et al.¹¹ examined the influence of various raster orientations on the tensile and impact strength of ABS printed parts. The study suggested that the 0° raster orientation has the highest mechanical performance than do the other raster orientations. Nidagundi et al.¹² conducted an experimental study on the relationship among ultimate tensile strength, surface roughness, dimensional accuracy and manufacturing time, orientation angle, and fill angle in FDM using Taguchi's S/N ratio.

To date, no study concerning the effect of fabrication conditions on creep performance has been found, and the relationships between these conditions and time-dependent deformation of processed material has not been studied yet. The aim of this article is to investigate the effect of fabrication conditions, such as slice thickness, raster-to-raster air gap, deposition angle, part print direction pressure, bead width, and number of perimeters on the flexural creep stiffness. Time-independent deformation of PC–ABS material was studied through a response surface definitive screening design and dynamic mechanical analyzer DMA 2980.

MATERIALS AND METHODS

The thermoplastic PC–ABS blend (density of 1098.89 kg/m³) was used in this study supplied by Stratasys, USA. A total of 13 specimens having the same dimensions of 60 × 12.5 × 3.5 mm (length × width × thickness) were fabricated using FDM Fortus 400 mc with different processing conditions as per the planned experimental design matrix shown in Table I. The specimen dimensions were selected as per test standard¹³ for Dynamic Mechanical Analysis.

Flexural creep stiffness tests were conducted using a three-point bending mode at the desired temperature of 80°C with a standard dynamic mechanical analysis instrument (DMA Model 2980TA, New Castle, USA). The flexural creep stiffness test was determined as a function of the time (creep time = 1800 s). Prior to the flexural creep stiffness measurement, the samples were equilibrated for 3 min to ensure that the sample had reached thermal equilibrium, and then the flexural creep stiffness was tested by applying a constant pressure of 12 MPa, which was within the linear viscoelastic deformation regimen and maintained for 1800 s. The load was then removed to allow the sample to recovery for 5400 s. The maximum value of flexural creep stiffness (FCS) test data has been reported for each specimen.

In this study, the response surface methodology based on definitive screening design was applied to optimize and investigate the influence of the fabrication parameters on the flexural creep stiffness. Six fabrication parameters— X_1 = slice thickness (0.127–0.3302 mm), X_2 = raster-to-raster air gap (0–0.5 mm), X_3 = deposition angle (0°–90°), X_4 = part print direction (0°–90°), X_5 = bead width (0.4572–0.5782 mm), and X_6 = number of perimeters (1–10)—were considered as input variables (Table I), and the flexural creep stiffness was determined as the response. In this study, the definitive screening design method has been applied for the first time to characterize the material and product performance in relation to the processing parameters. A definitive screening design is a new class of three-level experimental designs that can demonstrate higher efficiency than the classic response surface designs.¹⁴ A definitive screening design possesses several advantages for identifying the main effects, interaction effects, and quadratic effects with considerably less number of experiments. The main effects are confounded or aliased with quadratic effects and two-factor interactions, and all quadratic effects can be estimated effectively.¹⁵ A definitive screening design requires a minimum of $(2k + 1)$ runs, where k is the number of variables. Hence, an investigation on the effect of six fabrication parameters requires 12 experiments plus one center point. An analysis of variance (ANOVA) technique was used to verify the significance of the interaction effects between various parameters and the flexural creep stiffness.

RESULTS AND DISCUSSION

Model Fitting and Statistical Analysis

In this study, a mathematical model for the flexural creep stiffness was developed by fitting the experimental data with a quadratic regression model as expressed in Eq. 1:

$$\text{FCS} = \beta_0 + \sum_{i=1}^6 \beta_i X_i + \sum_{i=1}^6 \beta_{ii} X_i^2 + \sum_{i=1}^5 \sum_{j=i+1}^6 \beta_{ij} X_i X_j + \varepsilon \quad (1)$$

where FCS is the flexural creep stiffness; β_0 is the interception coefficient; β_i is the coefficient of linear effect; β_{ii} is the coefficient of the quadratic effect; β_{ij} is the coefficient of the interaction effect; X_i and X_j are independent variables; and ε is the random error.

The developed mathematical model for the flexural creep stiffness derived in terms of the actual factors is given by Eq. 2:

$$\begin{aligned} \text{FCS(MPa)} = & 902.487 - 29.387 \\ & \times \left[\frac{(x_1 - 0.2540)}{0.0762} \right] - 250.631 \\ & \times \left[\frac{(x_2 - 0.25)}{0.25} \right] + 28.794 \\ & \times \left[\frac{(x_3 - 45)}{45} \right] - 13.417 \times \left[\frac{(x_4 - 45)}{45} \right] \\ & - 8.331 \times \left[\frac{(x_5 - 0.5177)}{0.0605} \right] + 218.064 \\ & \times \left[\frac{(x_6 - 5)}{5} \right] + \left[\frac{(x_1 - 0.2540)}{0.0762} \right] \\ & \times \left\{ \left[\frac{(x_3 - 45)}{45} \right] \times 59.672 \right\} + \left[\frac{(x_4 - 45)}{45} \right] \\ & \times \left\{ \left[\frac{(x_4 - 45)}{45} \right] \times 30.083 \right\} \\ & + \left[\frac{(x_2 - 0.25)}{0.25} \right] \times \left\{ \left[\frac{(x_6 - 5)}{5} \right] \times 232.638 \right\} \\ & + \left[\frac{(x_5 - 0.5177)}{0.0605} \right] \\ & \times \left\{ \left[\frac{(x_6 - 5)}{5} \right] \times 67.608 \right\} \end{aligned} \quad (2)$$

Figure 1a and b graphically shows the ranking of the factors from most significant to least significant. Figure 1a is the Pareto chart of effects of standardized values of processing parameters on the flexural creep stiffness. It can be noticed that the process variables raster-to-raster air gap, number of perimeters, as well as the interaction between raster-to-raster air gap and number of perimeters have a more significant effect on the flexural creep stiffness than do the other terms. Figure 1b shows the estimated

regression coefficients and their significance for flexural creep stiffness. In statistical language, if the probability value (p value) is smaller than 0.05 (level of significance 5%), then the variable or interaction term is considered to have a significant effect on the response. In this case, as shown in Fig. 1b, the process variables (raster-to-raster air gap, number of perimeters, raster-to-raster air gap \times number of perimeters, bed width \times number of perimeters, slice thickness \times deposition angle, slice thickness, deposition angle, and part print direction) have p values smaller than 0.05 (at a confidence level of 95%). Hence, these process variables have a critical effect on the flexural creep stiffness and should be included in the fitted model. Insignificant variables and terms have been eliminated from the fitted model by using the backward elimination method. The backward elimination method is the most robust method for algorithmic model reduction because in this process all the variables and their terms will be given a chance to be included in the fitted model. In the backward elimination technique, the predictor variable with the highest partial p value, which is >0.1 , must be excluded from the fitted model as the p value <0.1 still makes a noise on the response. Therefore, the quadratic term (part print direction \times part print direction) with p value of 0.0602 and the individual variable (bead width) with p value of 0.0629 were included in the fitted model.

The diagnostic plot (Fig. 1c) is used to determine the capability of the developed model to fit the experimental data and to verify the required statistical assumptions. Figure 1c illustrates that the predicted values obtained from the developed model are in a very good agreement with the experimental values, which implies that the proposed model is adequate for this investigation.

Effect of the Fabrication Conditions

Figure 2 represents the 3D response surface plots illustrating the compositional interaction effects for various fabrication conditions over the design space. The interaction effect between part print direction and bead width is found to be interesting. It can be noticed from Fig. 2a that the maximum flexural creep stiffness can be achieved with the lowest value of bead width at zero degree of part print direction. This is because zero degree of part print direction exhibits a minimum stair-step effect, and the lowest value of bead width produces finer roads, which helps in achieving solid-filled interior regions of the part structure. Hence, the flexural creep stiffness improves remarkably. Figure 2b also shows that the lower value of slice thickness can improve the flexural creep stiffness because a lower slice thickness creates thinner rasters and roads, resulting in a minimum stair-stepping effect and hence better filled regions of the part structure. Figure 2b–d represents the flexural creep stiffness as a function

Table I. Experimental design matrix

Run	X_1	X_2	X_3	X_4	X_5	X_6	FCS(MPa)
1	0.127	0.25	90	0	0.4572	10	1103.282
2	0.3302	0.5	0	45	0.4572	10	925.4835
3	0.3302	0	45	0	0.5782	10	1212.572
4	0.3302	0.5	90	0	0.5177	1	302.5722
5	0.127	0.5	0	0	0.5782	5	690.8303
6	0.254	0	0	0	0.4572	1	1235.464
7	0.3302	0.25	0	90	0.5782	1	507.3044
8	0.127	0	0	90	0.5177	10	1214.309
9	0.127	0	90	45	0.5782	1	1090.207
10	0.3302	0	90	90	0.4572	5	1247.514
11	0.254	0.25	45	45	0.5177	5	870.9
12	0.127	0.5	45	90	0.4572	1	323.6737
13	0.254	0.5	90	90	0.5782	10	1214.309

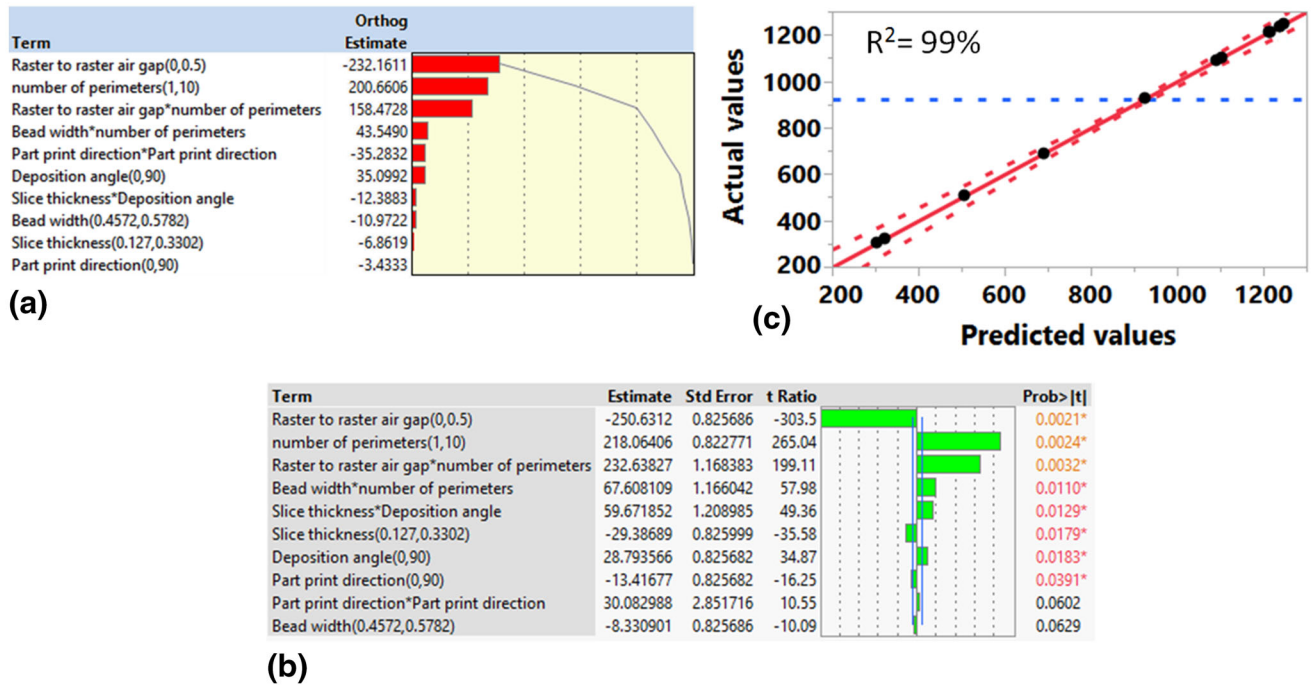


Fig. 1. (a) Pareto plot, (b) parameter estimates, and (c) scatterplot for predicted versus experimental values.

of raster-to-raster air gap combined with other parameters, which shows that raster-to-raster air gap is an effective parameter to improve the flexural creep stiffness of PC–ABS processed material. Figure 2b–d indicates that lower values of the raster-to-raster air gap can considerably maximize the flexural creep stiffness. This result is expected because zero air gap makes the rasters and bead widths touch each other within a region, leading to a stronger interior and dense microstructure. But an unexpected result can be seen in Fig. 2d. As a higher value of raster-to-raster air gap leads to poor mechanical properties and brittle structure, Fig. 2d demonstrates that it is still possible to obtain high

flexural creep stiffness by using a positive value of raster-to-raster air gap but using 10 perimeters. This is because the number of perimeter fills the part with external contours, internal contours, and internal raster fills. Thus, the number of perimeter minimizes the number of filling rasters, which can significantly reduce void formation. The scanning electron microscopy (SEM) microstructural images presented in Fig. 3a and b clearly show a highly dense microstructure of the part processed with 10 perimeters. This interesting finding has a significant industrial benefit not only to improve the mechanical properties but also to reduce the material consumption and processing time.

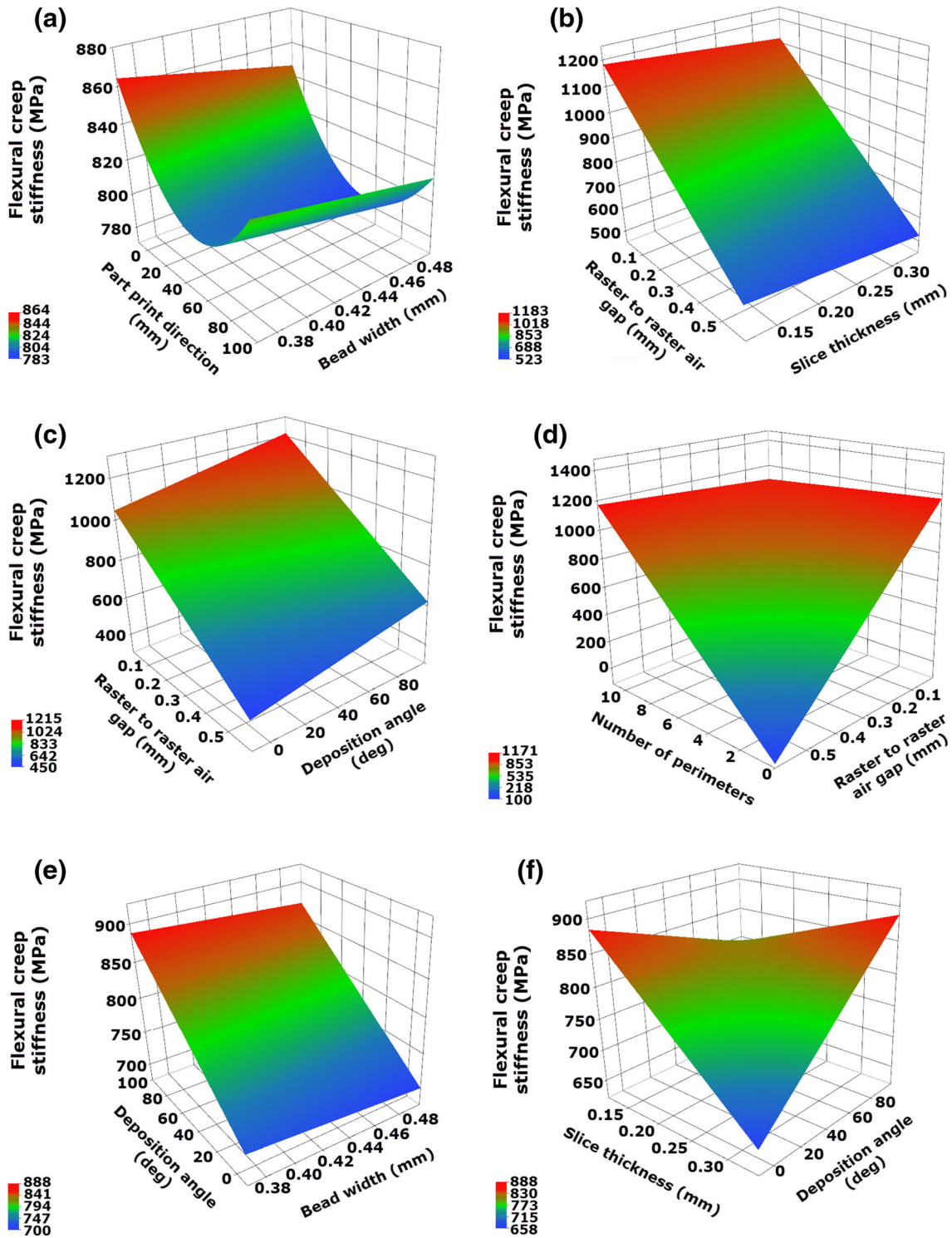


Fig. 2. 3D response surface plots showing the compositional–interaction effects between (a) part print direction and bead width, (b) raster-to-raster air gap and slice thickness, (c) raster-to-raster air gap and deposition angle, (d) number of perimeters and raster-to-raster air gap, (e) deposition angle and bead width, and (f) slice thickness and deposition angle.

Deposition angle also has a significant effect on the material response (Fig. 2c, e, and f). It can be seen from Fig. 2c, e, and f that the flexural creep stiffness increases with the increase in deposition angle. This is because higher values of deposition

angle lead to shorter raster length, and hence, the flexural creep stiffness improved significantly. Figure 2f illustrates that the interaction between slice thickness and deposition angle is interesting as this interaction plot plays a very important role in

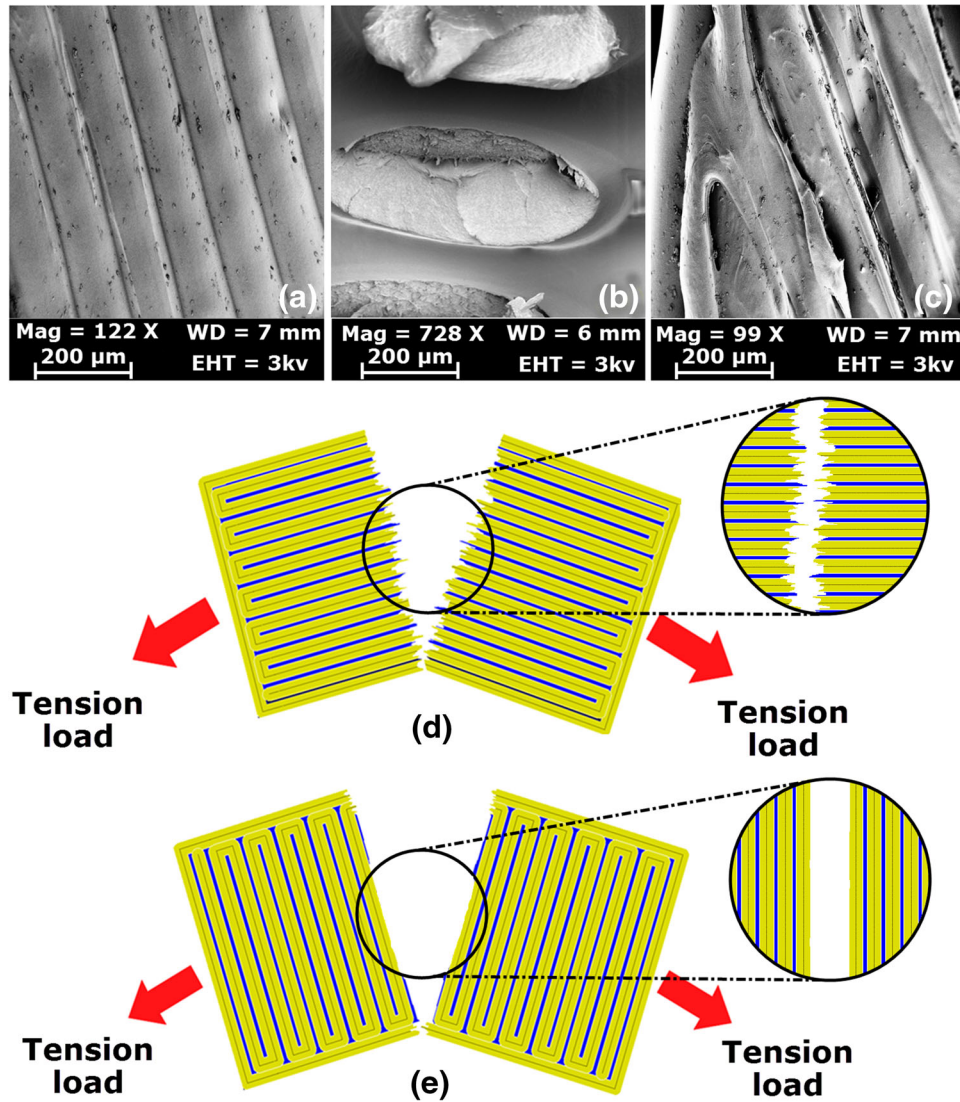


Fig. 3. SEM microstructural images for the sample processed with (a–b) 10 perimeters, (c) with a single perimeter and deposition angle of 45°, (d) failure mechanism of sample manufactured with disposition angle of 0°, and (e) failure mechanism of sample manufactured with disposition angle of 90°.

improving the flexural creep stiffness. It can be observed from Fig. 2f that the flexural creep stiffness can be higher (the same maximum value) either at the lowest values of slice thickness and deposition angle or at the highest values of slice thickness and deposition angle. This is because a deposition angle of 90° has a shorter raster length than does the deposition angle of 0°, which ideally improves the flexural creep stiffness. Nevertheless, Fig. 2f also shows that if the lowest values of slice thickness and deposition angle are used, then it is possible to obtain the highest flexural creep stiffness of the processed material and part. This is also an unexpected outcome through this study. To clarify these interesting results, Fig. 3d and e shows that if the material and the part are processed with the lower slice thickness along with a lower disposition angle, there would be many layers, fibers, and long

fiber reinforcement and the tension load would fracture many layers, fibers, and long fiber reinforcement. This can significantly enhance the deformation resistance and fracture of the processed part to the applied load. Hence, the part processed with a disposition angle of 0° (Fig. 3d) tends to be stronger than the part processed with a disposition angle of 90° (Fig. 3e). It is not advisable to process the part with a disposition angle of 45° as it leaves many empty gaps between the rounded corners and contours as shown in the SEM image presented in Fig. 3c.

Optimization of the Fabrication Conditions

In this study, the numerical optimization was conducted with Minitab statistical software version 17. The objective function is to maximize the

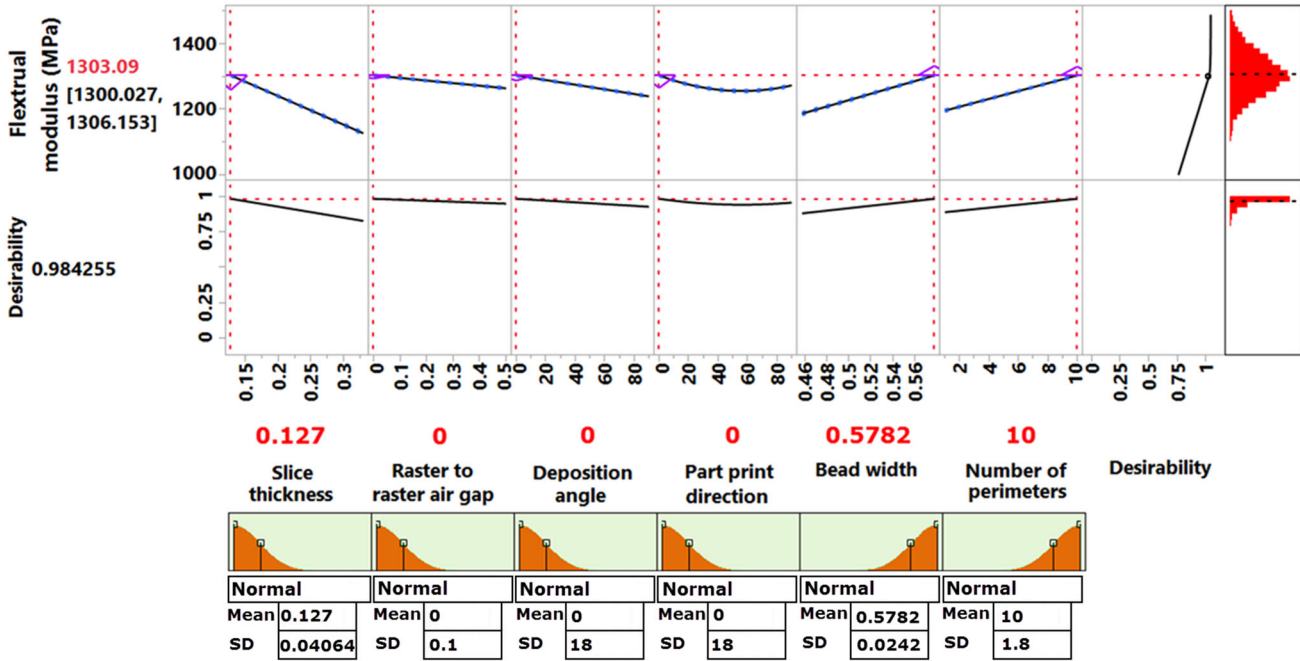


Fig. 4. Optimization plot for the optimal fabrication conditions.

Table II. Result of confirmation experiment

Response	Optimum level of process parameter						Predicted values	Actual values	Error
	A	B	C	D	E	F			
Flexural creep stiffness (MPa)	0.127	0	0	0	0.5782	10	1303.09	1298.412	-0.3589%

flexural creep stiffness in relation to the fabrication conditions detailed in Table I and to use the mathematical model developed in Eq. 2. As illustrated in Fig. 4, the optimum fabrication conditions were obtained with a slice thickness of 0.127 mm, zero air gap, deposition angle of 0°, part print direction of 0°, bead width of 0.5782 mm, and 10 perimeters, which predicted the flexural creep stiffness to be 1303.09 MPa with a high desirability of 0.984255.

The validity of the optimum levels of the process variables is then conducted through the confirmation experiment by manufacturing of three additional samples. Table II and Fig. 5 show a comparison between the predicted value of the flexural creep stiffness at the optimum levels of the process parameters and with the experimental value. The percentage of error is calculated through as shown in Eq. 3. It is clear from Table II and Fig. 5 that the maximum value of the flexural creep stiffness of 1298.412 MPa was obtained through confirmation experiments and that a small variation can be observed between the predicted and the experimental value. This indicates that the pre-

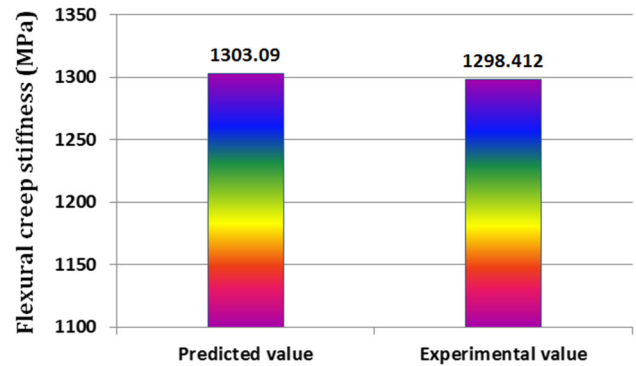


Fig. 5. Comparison of predicted flexural creep stiffness versus actual values.

dicted value is in very good agreement with the experimental value. Therefore, the applicability and suitability of the model employed and the success of definitive screening design in optimizing the FDM process conditions are proven:

$$\begin{aligned} & \text{Percentage of error}(\%) \\ &= \left| \frac{\text{Actual value} - \text{Predicted value}}{\text{Predicted value}} \right| \times 100 \quad (3) \end{aligned}$$

CONCLUSION

The relationships between the fabrication conditions and the flexural creep stiffness of PC–ABS material processed by FDM were investigated. The slice thickness of 0.127 mm, zero air gap, deposition angle of 0°, part print direction of 0°, bead width of 0.5782 mm, and 10 perimeters are found to be the optimum fabrication conditions for improving the flexural creep stiffness. A response surface definitive screening design adopted in this study further substantiates the robust nature of this approach with respect to characterizing the material and product to a desired range of mechanical properties. The developed model is useful in industry for evaluation of the flexural creep stiffness without conducting multiple experiments. The influences of the fabrication parameters on the material response and product quality remain an interesting issue for future studies.

REFERENCES

1. T.M. Wang, J.-T. Xi, and Y. Jin, *Int. J. Adv. Manuf. Technol.* 33, 1087 (2007).
2. O.A. Mohamed, S.H. Masood, and J.L. Bhowmik, *Adv. Manuf.* 3, 42 (2015).
3. M. Avalle, M. Peroni, and A. Scattina, *Latin Am. J. Solids Struct.* 7, 41 (2010).
4. M. Al-Haik, M. Hussaini, and H. Garmestani, *Int. J. Plast.* 22, 1367 (2006).
5. M.S. Hossain, J. Ramos, D. Espalin, M. Perez, and R. Wicker, *International Solid Freeform Fabrication Symposium: An Additive Manufacturing Conference* Austin, TX, 380 (2013).
6. J. Torres, J. Coteló, J. Karl, and A.P. Gordon, *JOM* 67, 1183 (2015).
7. F. Knoop and V. Schoeppner, *26th Annual International Solid Freeform Fabrication Symposium*, Austin, TX, 935 (2015).
8. C. Basavaraj and M. Vishwas, *IOP Conf. Ser. Mater. Sci. Eng.* 149, 012035 (2016).
9. O.A. Mohamed, S.H. Masood, and J.L. Bhowmik, *Appl. Math. Model.* 40, 10052 (2016).
10. C.A. Griffiths, et al., *Proc. Inst. Mech. Eng. Part B J. Eng. Manuf.* 10, 1177 (2016).
11. O. Es-Said, J. Foyos, R. Noorani, M. Mendelson, R. Marloth, and B. Pregger, *Mater. Manuf. Process.* 15, 107 (2000).
12. V.B. Nidagundi, R. Keshavamurthy, and C. Prakash, *Mater. Today Proc.* 2, 1691 (2015).
13. ASTM D5418-07 Standard Test Method for Plastics: Dynamic Mechanical Properties: In Flexure (Dual Cantilever Beam), ASTM International, West Conshohocken (2007).
14. B. Jones and C.J. Nachtsheim, *J. Qual. Technol.* 43, 1 (2011).
15. B. Jones and C.J. Nachtsheim, *J. Qual. Technol.* 45, 121 (2013).